

	SAKARYA UNIVERSITY JOURNAL OF SCIENCE		 SAKARYA UNIVERSITY
	e-ISSN: 2147-835X http://www.saujs.sakarya.edu.tr		
	Recieved	Accepted	
	2017-10-17	2017-12-12	10.16984/saufenbilder.344752

Determination of Solubility Characteristic of (Bi, Gd) Substitution in Bi-2223 Inorganic Compounds

Yusuf Zalaoglu*¹

ABSTRACT

In this study, it is examined the significant variations in the superconducting, electrical and structural belongings of Bi-site Gd nanoparticle substituted Bi-2223 crystal. The $\text{Bi}_{2.0-x}\text{Gd}_x\text{Sr}_{2.0}\text{Ca}_{2.1}\text{Cu}_{3.2}\text{O}_y$ ($0 \leq x \leq 0.3$) materials obtained with the standard solid state reaction technique are characterized by dc resistivity (ρ -T), X-ray diffraction (XRD) and transport critical current density (J_c) measurements. Moreover, all experimental findings as regards room temperature resistivity, residual resistivity, critical transition temperatures ($T_c^{\text{onset}} - T_c^{\text{offset}}$), crystallinity, lattice constant parameters, average crystallite size, phase fraction and strength quality of interaction between superconducting grains in the Bi-2223 ceramics declare that the structural, electrical and superconducting characteristics degrade systematically with the ascending of the Gd substitution level in the Bi-2223 samples. Furthermore, the major reason of the reduction trend observed especially in the electrical and superconducting features is in relation with the hole localization problem in the Cu-O₂ layers. In this regard, grain boundary weak connections, dislocations and defects in the matrix considerably ascend with the enhancement of Gd nanoparticle substitution level. As seen from XRD measurements, it is clearly determined that there seems to be a decrement in the Bi-2223 phase with the enhancement of Gd inclusions up to the substitution amount of $x=0.1$. After this critical point, new characteristics peaks of Gd₂O₃ appear and measurement findings rapidly diminish to the minimum values. This substitution level emphasizes that the solubility limit of Gd is noted to be $x=0.1$ for Bi-2223. Likewise, the regular decrement observed c-axis length, critical current density and grain size favors the regular retrogression of the superconducting characteristics.

Keywords: Bi-site Gd substitution, Bi-2223 superconducting matrix, solubility limit, XRD

* Corresponding Author

¹ Osmaniye Korkut Ata Üniversitesi Fen-Edebiyat Fakültesi, Fizik Bölümü, OSMANİYE-yzalaoglu@osmaniye.edu.tr

1. INTRODUCTION

In the last decade, the discovery of superconductors has inspired great interest in the science world due to not only having zero electrical resistance but also behaving as a perfect diamagnet below the critical temperature. Additionally, researchers have concentrated their fundamental investigations related with the superconducting materials on high temperature superconductors (known as Type-II superconductor) [1]. Especially, within the Type-II superconductors, it is pointed out that studies are centered on the first type high temperature superconducting system without rare earth element, BSCCO [2-8]. This effective superconducting mechanism is composed of a generalized chemical formula $\text{Bi}_2\text{Sr}_2\text{Ca}_{y-1}\text{Cu}_y\text{O}_x$ where y value corresponds to 1, 2 and 3, respectively. What is more, the superconducting transition temperatures of three superconducting phases are depicted by 20, 95 and 110 K, respectively [9]. Nevertheless, it is experimentally hard to acquire Bi-2223 high temperature phase because of excessive complexity of the reaction and the presence of Bi-2201 and Bi-2212 superconducting phases [10]. Furthermore, several remarkable surveys are conducted consistently to enhance the magnetic, mechanical, electrical and superconducting belongings of the most important member of BSCCO superconducting family. Besides, these surveys carried out by changing the heat treatment mechanism, type and quantity of doping material, composition of superconducting sample and preparation techniques [11-19]. Generally, the major of the studies done so as to augment the superconducting characteristics of BSCCO is the addition or substitution process of the elements to the matrix. Recently, nanoparticle addition or substitution processes to Bi-2223 phase is condensed day by day with the help of the developing technology [20-30]. Additionally, introduction of nanoparticles in the high temperature superconducting systems has attracted significant attention due to the fact that these particles are thought as simply controlled and productive instrument to develop superconducting characteristics. That is to say, if nanoparticles are added to the matrix, they can be easily adopted into the system and much more among the grains with respect to the micro size doping material. It is said that this statement can

be sourced from the very small size of nanoparticles [31-34]. On the other hand, although the studies associated with the Gd foreign particles to Bi-2223 matrix are available in literature [35-44], there are not any papers related with the partial replacement of Gd nanoparticle on Bi-site in Bi-2223. In this current work, we analyzed the impact of Gd nanoparticle substitution on Bi-site in Bi-2223 crystal structure (not including Pb element) and the solubility limit of trivalent Gd nanoparticles throughout the system. It is clearly found that the critical transition temperatures, grain size of the samples, hole concentration and lattice parameter c systematically decreased with the increment of Gd nanoparticle addition. Also, the solubility limit of this system is obtained as $x=0.1$ due to the fact that new characteristics peaks defined as Gd_2O_3 is observed after this limit value by means of the XRD findings.

2. EXPERIMENTAL DETAILS

The $\text{Bi}_{2.0-x}\text{Gd}_x\text{Sr}_{2.0}\text{Ca}_{2.1}\text{Cu}_{3.2}\text{O}_y$ ($0 \leq x \leq 0.3$) superconducting ceramics are conveniently prepared from the mixtures of chemical powders provided from Alfa Aesar Co., Ltd. with 99.99 % such as Bi_2O_3 , Gd_2O_3 , SrCO_3 , CaCO_3 , CuO . This sensitive preparation process is occurred in atmospheric air via the traditional solid state reaction technique. The starting carbonates, oxides are firstly ground in agate mortar about half-hour so as to get smaller particle sizes from coarse powders. Then, the chemicals are blended in a grinding machine about 8 hours. The mixture is pelletized into a rectangular bar ($1.5 \times 0.5 \times 0.2 \text{ cm}^3$) under 300 MPa constant pressure at room temperature. The pellets are calcined at 800 °C in a Protherm programmable tube furnace during the duration of 24 h with 3°C/min heating and 5°C/min cooling rates. The rectangular pellets being subjected to calcination process are reground about 1.5 h in the agate mortar and again pressed under 300 MPa constant pressure at room temperature. The samples prepared are depicted as [Gd--0], [Gd--1], [Gd--2], [Gd--3], [Gd--4], [Gd--5] and [Gd--6] with the increment Gd stoichiometry ($x=0, 0.01, 0.03, 0.05, 0.07, 0.1, 0.3$) respectively. The electrical properties of the solid superconducting ceramics obtained sensitively are measured by means of dc resistivity-temperature measurements with dc current of 5 mA. Moreover, the measurements are carried out between the temperature range of 70

K and 125 K by conventional four probe technique in the He gas contact cryostat under vacuum. The experimental measurements of this four probe technique are carried out with programmable current source and nanovoltmeter. Also, the measurement findings of the samples are taped as resistance vs. temperature curves with the help of the Labview software. Also, the transport critical current examinations are performed by similar process with the resistance measurements. Besides, the transport critical current findings are obtained by four probe contact method including a homemade system equipment with the accuracy of ± 0.01 K at the liquid nitrogen temperature in zero magnetic field. As for the XRD evidences, the measurements of samples prepared are performed via Rigaku Multiflex+XRD 2kW diffractometer with $\text{CuK}\alpha$ target for the monochromatic beam with 1.54 \AA wavelength at room temperature. The data are collected over the diffraction angle in the range of $2\theta = 3\text{--}60^\circ$ with a scan speed of $3^\circ/\text{min}$.

3. RESULTS and DISCUSSIONS

3.1. Dc Resistivity Analysis

In this section, it is examined the several experimental findings such as room temperature resistivity, the degree of the broadening, offset and onset transition temperatures obtained from dc resistivity curves in the temperature interval starting from 70 K and ending with 125 K so as to reveal the changes in the superconducting and electrical features of partial replacement of Gd nanoparticles in Bi-site in Bi-2223 crystal structure in detail. Firstly, the residual resistivity ratio (RRR) and temperature-independent residual resistivity (ρ_0) parameters are determined from electrical resistivity curves. Also, the first parameter obtained from the conventional extrapolation method refers to the defects derived from either scattering centers or the grain boundary weak-links [45, 46], whereas another one found from the ratio of $\rho_{300\text{K}}/\rho_{115\text{K}}$ is an effective method so as to identify the sample quality [47]. These parameters for the specimens prepared are numerically displayed in Table 1.

Table 1. Electrical resistivity evidences of the materials prepared in this work

<i>Samples</i>	$T_c^{\text{onset}}(\text{K})$	$T_c^{\text{offset}}(\text{K})$	$\Delta T_c(\text{K})$	ρ_0 ($\text{m}\Omega.\text{cm}$)	$\rho_{300\text{K}}$ ($\text{m}\Omega.\text{cm}$)	$\rho_{115\text{K}}$ ($\text{m}\Omega.\text{cm}$)	<i>RRR</i> ($\rho_{300\text{K}}/\rho_{115\text{K}}$)	<i>Hole Concentration, P</i>
[Gd--0]	111.1	109.3	1.8	12.91	94.36	45.10	2.09	0.1512
[Gd--1]	109.3	107.2	2.1	20.66	100.60	52.08	1.93	0.1424
[Gd--2]	107.7	105.3	2.4	26.21	105.03	57.32	1.83	0.1373
[Gd--3]	105.9	102.5	3.4	39.87	109.14	66.76	1.63	0.1313
[Gd--4]	104.1	100.2	3.9	47.56	111.50	70.26	1.59	0.1272
[Gd--5]	98.6	89.7	8.8	62.93	114.07	82.66	1.38	0.1127
[Gd--6]	96.2	83.1	13.1	78.30	117.91	93.48	1.26	0.1056

Likewise, it is obviously observed from table given above that ρ_0 values systematically increases from $12.91 \text{ m}\Omega.\text{cm}$ to $78.30 \text{ m}\Omega.\text{cm}$ with the augmentation of Gd substitution level. This consequence appeared reveals with the enhancement of random defects and impurity scattering concerning with the stacking faults,

voids, the grain boundaries, micro defects in the consecutively Cu–O₂ planes [48]. Moreover, as seen clearly from RRR values from Table 1, it is said that the pristine has the best quality material among the samples produced; therefore, it exhibits the best conductivity characteristic. Moreover, the dc electrical resistivity measurements are depicted in Figure 1.

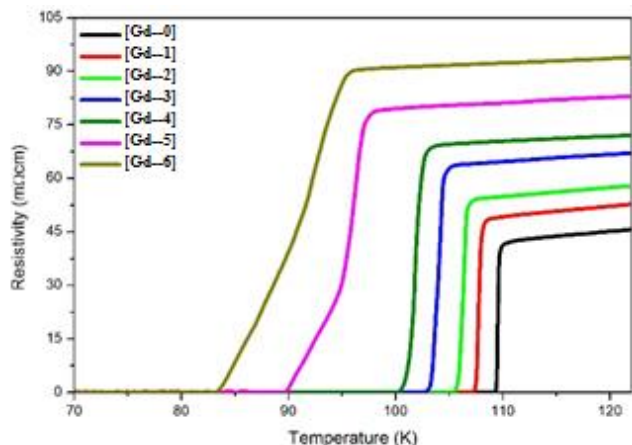


Figure 1. Electrical resistivity vs. temperature graphs between the temperature range of 70 K and 125 K for Gd substituted Bi-2223 crystal systems

In figure, it is clearly pointed out that the maximum $T_c^{offset}(T_c^{onset})$ value of 109.3 K (111.1 K) is determined for the virgin sample whereas the [Gd--6] material has the minimum values 96.2 and 83.1 K for T_c^{onset} and T_c^{offset} values, respectively. Moreover, it is easily observed that not only onset critical transition (T_c^{onset}) but also offset critical transition (T_c^{offset}) values systematically degrade with the augmentation of the Gd foreign particles, exhibiting that the electrical and superconducting characteristics of the crystal system harshly damages. Similarly, as seen from the variations of the critical transition temperature values displayed in Table 1, the variance T_c^{offset} in value is much more than T_c^{onset} value in the existence of Gd inclusion in the polycrystalline Bi-2223 system. The fundamental reason why the critical temperature (T_c^{offset}) reduces rapidly may be due to not only Cooper pair breaking mechanism as regards Abrikosov-Gorkov theory (generally called as localization problem) but also average grain size because of the improvement in the weakening of the intergrain coupling and porosity [7, 49]. Further, the remarkable decrement observed at critical temperatures is stemmed from the existence of the grain boundary weak-interactions between Cu-O₂ planes in the Bi-2223, distortion and artificial random defects [50–53]. Similarly, it is remarkably seen that the

increased critical temperature variations with the dopant level causes the degradation of the degree of broadening. Moreover, the smallest degree of broadening value of 1.8 K represents the virgin while the values of degree of broadening increase progressively from 2.1 K to 13.1 K with the augmentation of Gd substitution into the Bi-2223 matrix. At the same time, the main reason of the statement mentioned above is that Gd inclusions inserted into the superconducting matrix did not enhance the growth of the 2223-high phase. Furthermore, it is to be mentioned here that the variation of homogeneities in the oxidation states causes the regular increment in the degree of broadening. Besides, it can be mentioned that the existence of the Gd substitution into Bi-2223 inorganic compounds damages the metallic character owing to the diminishment of the mobile hole carrier concentration in the Cu-O₂ layers and metallic interaction between the grains. Additionally, these factors lead to the increasing room temperature resistivities with the improvement of Gd substitution amount. In numerically, whereas the minimum room temperature resistivity (ρ_{300K}) value is determined to be about 94.36 mΩ.cm for the virgin inorganic material, the maximum value is 117.91 mΩ.cm for the [Gd--6] material.

3.2. XRD Measurement Findings

As for the XRD examination, the crystal structure with crystallinity, texturing, crystallite size, lattice cell parameters and phase purity related to superconducting materials produced are sensitively analyzed. Further, the experimental data are derived from XRD between the angle range of 3° and 60° at room temperature. What's more, XRD patterns of the samples belonging to the pristine and Gd substituted Bi-2223 inorganic samples are indicated in Figure 2. As observed figure, the XRD patterns of the specimens prepared include not only Bi-2212 phase but also Bi-2223 phase. In figure, as “H” character specifies the peaks belonging to the 2223-high phase, 2212-low phase are inferred by “L” letter. Moreover, the corresponding (hkl) Miller indices belonging to samples prepared are displayed in Figure 2.

Hence, the most striking point being visible from XRD patterns that the solubility limit of the Gd foreign particle in the Bi-2223 crystal is determined to be about $x=0.1$. Additionally, the relative percentages with respect to 2223-high and 2212-low phases are analyzed with the aid of the equations as follow

$$f_{(2223)} = \frac{\sum I_{2223(hkl)}}{\sum I_{2223(hkl)} + \sum I_{2212(hkl)}} \quad (1)$$

$$f_{(2212)} = \frac{\sum I_{2212(hkl)}}{\sum I_{2212(hkl)} + \sum I_{2223(hkl)}} \quad (2)$$

In this equation, I is in association with the peak intensity of the phase observed in the XRD measurement. The findings are indicated in Table 2. As observed from the table, the 2223-high phase regularly suppresses from 90.7 to 77.5 % with the augmentation in the Gd substitution point up to the amount of $x = 0.07$, and just about to start from this critical point, this value immediately decreases towards to the value of 54.7 % along with the enhancement of substitution amount. Nevertheless, the relative percentage related to the Bi-2212 phase ascends systematically to 45.3 %. It is clearly observed that higher intensities in XRD curves are achieved from the diffraction obtained from (00l) planes in comparison with the other plane reflections. Further, the substitution level of the Gd foreign particle in the crystal system strongly affects the conventional lattice parameters obtained with the help of the least square method. Besides, the variations observed in the lattice parameters can be expressed as the peak-shifts of partial diffraction planes. Also, thanks to this phenomena, it can be robustly presented that Gd insets smoothly introduce into the partial Bi sites of the Bi-2223 superconducting matrix. Apart from that, this situation mentioned above can be expressed with the meaningful explanation. Despite of the fact that Gd and Bi have different electron configurations at the outer shell, they have the same chemical valence. Also, Gd inclusion has an electron configuration with the ending of $5d^1 6s^2$ while $6s^2 6p^3$ sequence presents the electronic configuration outer atomic electron for Bi atom. As Bi and Gd atoms come across with the oxygen atoms of Bi-sites, Gd^{+3} atoms easily come together with the oxygen atoms via dsp hybrid orbital. On the contrary side, Bi atoms also integrate with the surrounding oxygen atoms

in order to form p-p bond. Also, extra energy is required for the p-p bond formation process for Bi atoms. In other words, in the orbital hybrid process, p-p bond formation requires extra energy as compared to the dsp orbital hybrid, and therefore La atoms much easily integrate with the surrounding oxygen atoms of Bi-sites. Hereby, lack of oxygen is observed in Bi-O planes and O atoms swiftly start to go towards into BiO layers from neighboring BiO planes and SrO planes. Hence, the distances of the Cu-Ca-Cu and Ca-Sr sites enlarge and the interlayer distances of the Sr-Bi, Bi-Bi and Sr-Bi-Bi-Sr sites decrease, bringing about contracting the c-axis parameter [57-61]. On the other hand, the increment observed a length is related that the ionic radius of the inclusions substituted to the matrix (Gd^{+3}) is much larger than that of Bi^{+3} . Moreover, as you probably know, a lattice parameter is controlled with the Cu-O bond length in the Cu-O₂ layers. It is thought that these layers are significantly precious because of being in charge of the sizes in the basal planes [58, 59]. Similarly, the hole compensation mechanism is happened owing to the increment of effective Cu valence, and then a lattice parameter increases [55-56, 62]. Based on the numerical values of the lattice parameters (Table 2), a parameter is observed to ascend from 5.32 Å (for the pure material) to 5.43 Å (for the [Gd--6] sample) while the c-axis parameter is found the decrement trend from 36.92 Å (for pristine) to 30.55 Å (for [Gd--6] sample). Further, the crystallite size of virgin and (Bi, Gd)-2223 superconducting materials is performed with the aid of the XRD patterns by using the formula given below [63];

$$t = 0.941\lambda / B \cos \theta_B \quad (3)$$

Here, t represents the crystal thickness, λ shows the wavelength of the XRD, θ_B denotes the Bragg angle, B illustrates the full width at half maximum (FWHM) of the Bragg peak. Also, B is expressed as following relation

$$B^2 = B_m^2 - B_s^2 \quad (4)$$

where B_s remarks the half width of the standard material in radians. In addition, the grain size values of all samples calculated with the help of the XRD patterns diminish with the increment of Gd substitution into Bi-2223 matrix.

Table 2. J_c and XRD evidences of the pure and inorganic bulk Gd substituted materials

Samples	a (Å)	c (Å)	Volume fraction ($\approx\%$)		Average grain size (nm)	J_c ($A.cm^{-2}$)
			2223	2212		
[Gd--0]	5.32	36.92	90.7	9.3	61.5	607
[Gd--1]	5.34	36.41	86.5	13.5	59.1	521
[Gd--2]	5.36	36.17	84.8	15.2	56.4	468
[Gd--3]	5.37	35.56	82.3	17.7	52.9	411
[Gd--4]	5.37	33.76	77.5	22.5	49.6	339
[Gd--5]	5.41	31.12	60.5	39.5	47.1	246
[Gd--6]	5.43	30.55	54.7	45.3	46.4	232

Numerically, as seen from Table 2, it is emphasized that the grain size values tend to retrogress systematically from 61.5 nm to 46.4 nm with the increment of the substitution level. Also, it is approved that this decline is related with the decrement of the crystallinity and interaction between the grains.

3.3. Hole-Carrier Concentration Survey

As for the hole-carrier concentrations, P , are computed with the aid of equation as follows [64]:

$$P = 0.16 - \left[\left(1 - \frac{T_c^{offset}}{T_c^{max}} \right) / 82.6 \right]^{1/2} \quad (5)$$

where T_c^{max} value is approved as 110 K for 2223-high phase [65] and T_c^{offset} is received from Table 1. In this regard, it is attributed from Table 1 that hole-carrier concentration (P) values are regularly degrade starting from 0.1512 and ending to 0.1056 with the enhancement of Gd inclusions. (Figure 4(a)) In addition to this, the change of hole-carrier concentration with respect to Gd-content and superconducting critical transition temperature (T_c^{offset}) are shown in Figure 4(b), respectively.

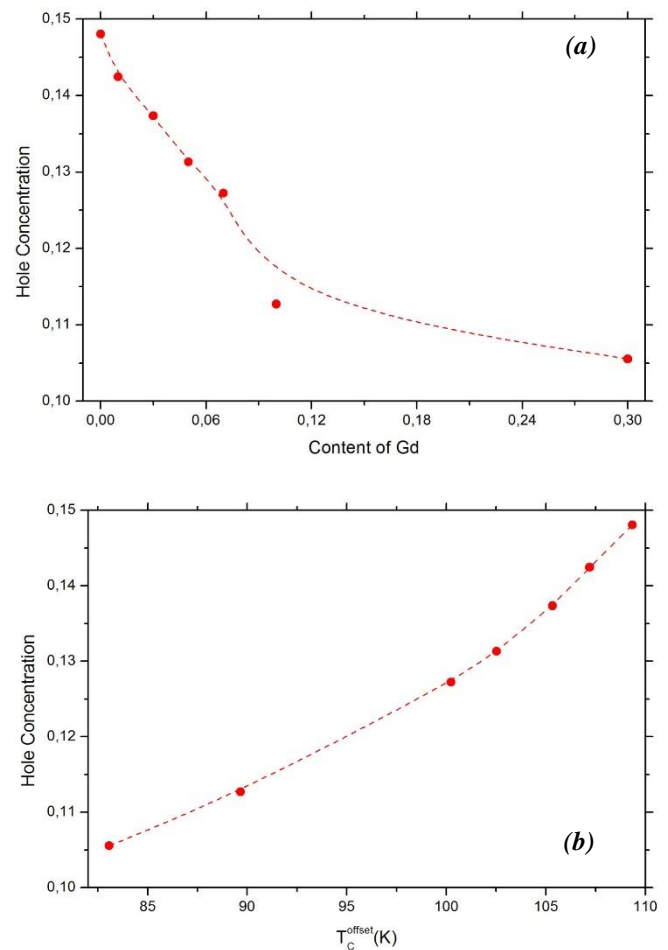


Figure 4. (a) Hole-carrier concentration vs. Gd content graph; (b) Hole-carrier concentration vs. T_c^{offset} for all the superconducting specimens

As can be seen from figures, while the hole carrier concentration decreases with increasing Gd substitution, the parabolic relationship is observed between the T_c^{offset} and hole-carrier concentration values. Thus, the enhancement of Gd addition to Bi-2223 superconducting system significantly diminishes the hole carrier

concentration, bringing about the fact that the superconducting characteristics of the crystal system systematically decreases.

3.4. Transport Critical Current Density

The self-field critical current density (J_c) surveys of the Bi-2223 matrix is evaluated by means of Figure 5(a). As seen from figure, the self-field J_c value descends regularly with the increment Gd substitution to the system. As seen from numeric values in Table 2, the maximum current density value is obtained as 607 A.cm^{-2} for undoped sample while the [Gd--6] sample indicates minimum J_c value of 232 A.cm^{-2} at 77 K (called as boiling point of liquid nitrogen). This retrogression noted in J_c can be explained with the increment of the grain boundaries resistance, secondary phases, porosity, de-orientation of Bi-2223 grains with the addition of Gd inclusions and the weak links between the superconducting grains [53, 56]. Besides, the association between the critical current densities and transition temperatures of the samples prepared is plotted in Figure 5(b). As seen from Figure 5(b), T_c and J_c values descends with the enhancement of Gd foreign particles. On the other hand, it is robustly found that J_c value is more sensitive to the variation of Gd inclusion with respect to the transition temperatures.

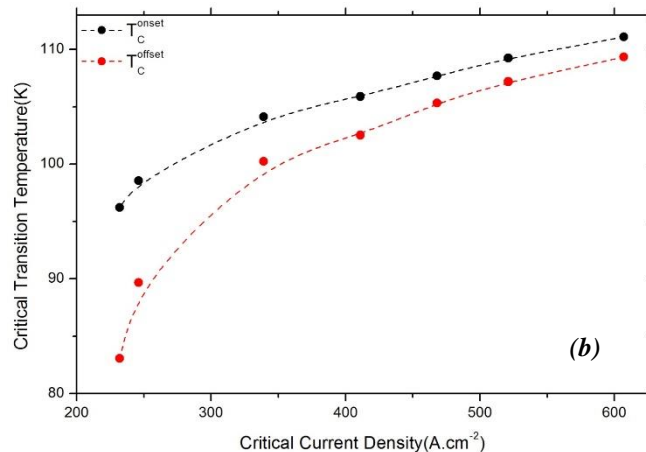
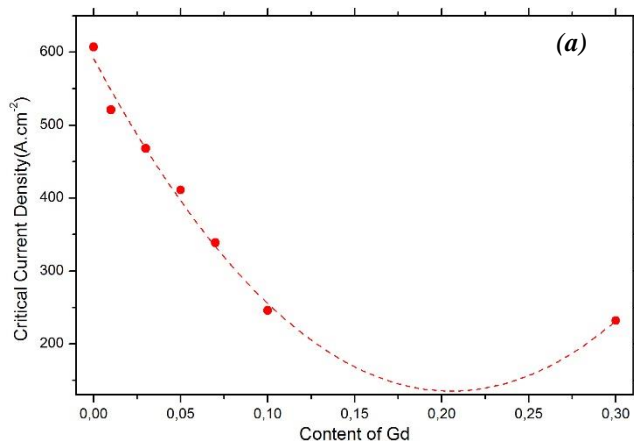


Figure 5. (a) Variation of J_c vs. Gd content graph; (b) Variation of T_c values vs. J_c graph for the poly-crystallized materials

4. CONCLUSION

In this exhaustive study, the superconducting and structural belongings of Gd substituted on Bi-site of $\text{Bi}_{2.0-x}\text{Gd}_x\text{Sr}_{2.0}\text{Ca}_{2.1}\text{Cu}_{3.2}\text{O}_y$ ($0 \leq x \leq 0.3$) superconductors obtained with the aid of the conventional solid-state reaction method as regards $x=0, 0.01, 0.03, 0.05, 0.07, 0.1$ and 0.3 is investigated via R-T, I-V and XRD findings. Moreover, it is tempting to speculate that Gd concentration level precisely affects the all characteristic properties. As is seen from dc electrical resistivity results, the metallic character and room temperature conductivity are destroyed with the presence of the Gd nanoparticles in matrix. This statement can be occurred in consequence of ascending disorders of metallic interaction and the regression in the hole carrier concentration occurred in the Cu-O stacked layers. Moreover, the T_c^{onset} and T_c^{offset} values decrease significantly owing to the fact that the increment of grain boundary weak-links, distortion and artificial random defects are taken place between superconducting slabs in the matrix. Besides, it is obtained that transport critical current densities decrease from 607 A.cm^{-2} to 232 A.cm^{-2} with the increment of Gd substitution on Bi-site, respectively. As for the XRD consequences obtained from the samples prepared, it can be clearly observed that Gd foreign particles do not provide 2223-high phase continuity with ascending amount of x because of the regression in the peak intensities. Additionally, the relative percentage of the 2223-high phase typically diminishes from 90.7 % until 54.7 %. On the other hand, new characteristic peaks related to the Gd_2O_3 tetragonal phase is

observed in XRD graphs for $x=0.3$ at $2\theta= 28.40^\circ$ and 33.23° . If Gd_2O_3 tetragonal phase is seen from XRD findings in this way, it is said that the solubility limit of the Gd inclusions in the Bi-2223 is about $x=0.1$. Besides, as the lattice parameter values are analyzed from XRD patterns, not only lattice parameter a enhances but also the c parameter systematically descends with the increment of the Gd substitution. After all, it is important to mention here that the grain sizes of the materials calculated via XRD patterns diminish from 61.5 nm to 46.4 nm with the Gd substitution, verifying the deterioration of the interaction between the grains and crystallinity between the grains.

REFERENCES

- [1] V.L. Ginzburg, E.A. Andryushin, Superconductivity, Revised ed. World Scientific Pub. Co. Inc., 2004.
- [2] M. Hiroshi, T. Yoshiaki, F. Masao and A. Toshihisa, "A new high- T_c oxide superconductor without a rare earth element," *Japanese Journal of Applied Physics Part 2-Letters*, vol. 27, no. 2, pp. L209–L210, 1988.
- [3] P. A. Lee and N. Read, "Why is T_c of the oxide superconductors so low," *Physical Review Letters*, vol. 58, no. 25, pp. 2691–2694, 1987.
- [4] K. Levin, J. H. Kim, J. P. Lu and Q. Si, "Normal state properties in the cuprates and their Fermi-liquid based interpretation," *Physica C*, vol. 175, no. 5–6, pp. 449–522, 1991.
- [5] G. Yildirim, M. Dogruer, F. Karaboga and C. Terzioglu, "Formation of nucleation centers for vortices in Bi-2223 superconducting core by dispersed Sn nanoparticles," *Journal of Alloys and Compounds*, vol. 584, pp. 344–351, 2014.
- [6] O. Gorur, C. Terzioglu, A. Varilci and M. Altunbas, "Investigation of some physical properties of silver diffusion-doped $YBa_2Cu_3O_{7-x}$ superconductors," *Superconductor Science & Technology*, vol. 18, no. 9, pp. 1233–1237, 2005.
- [7] M. B. Turkoz, S. Nezir, C. Terzioglu, A. Varilci and G. Yildirim, "Investigation of Lu effect on $YBa_2Cu_3O_{7-\delta}$ superconducting compounds," *Journal of Materials Science-Materials In Electronics*, vol. 24, no. 3, pp. 896–905, 2013.
- [8] Y. Zalaoglu, G. Yildirim, C. Terzioglu and O. Gorur, "Detailed analysis on electrical conduction transition from 2D variable range hopping to phonon-assisted 3D VRH mechanism belonging to Bi-site La substituted Bi-2212 system," *Journal of Alloys and Compounds*, vol. 622, pp. 489–499, 2015.
- [9] A. I. Abou-Aly, M. M. H. Abdel Gawad and R. Awad, "Improving the physical properties of (Bi, Pb)-2223 phase by SnO_2 nano-particles addition," *Journal of Superconductivity and Novel Magnetism*, vol. 24, no. 7, pp. 2077–2084, 2011.
- [10] M. Takano, J. Takada, K. Oda, H. Kitaguchi, Y. Miura, Y. Ikeda, Y. Tomii and H. Mazaki, "High- T_c phase promoted and stabilized in the Bi, Pb-Sr-Ca-Cu-O system," *Japanese Journal of Applied Physics Part 2-Letters*, vol. 27, no. 6, pp. L1041–L1043, 1988.
- [11] C. Y. Shieh, Y. Huang, M. K. Wu and C. Y. Huang, "Preparation of single high- T_c phase Bi-Pb-Sr-Ca-Cu-O superconductor by the EDTA precursor solution method," *Physica C*, vol. 185–189, pp. 513–514, 1991.
- [12] S. A. Halim, A. K. Saleh, H. Azhan, S. B. Mohamed, K. Khalid and J. Suradi, "Synthesis of $Bi_{1.5}Pb_{0.5}Sr_2Ca_2Cu_3O_y$ via sol-gel method using different acetate-derived precursors," *Journal of Materials Science*, vol. 35, no. 12, pp. 3043–3046, 2000.
- [13] A. Tampieri, G. Celotti, S. Lesca, G. Bezzi, T. M. G. la Torretta and G. Magnani, "Bi(Pb)-Sr-Ca-Cu-O(2223) superconductor prepared by improved sol-gel technique," *Journal of the European Ceramic Society*, vol. 20, no. 2, pp. 119–126, 2000.
- [14] I. Hamadneh, A. Agil, A. K. Yahya and S. A. Halim, "Superconducting properties of bulk $Bi_{1.6}Pb_{0.4}Sr_2Ca_{2-x}Cd_xCu_3O_{10}$ system prepared via conventional solid state and coprecipitation methods," *Physica C*, vol. 463–465, pp. 207–210, 2007.
- [15] E. Yanmaz, I. H. Mutlu, S. Nezir and M. Altunbas, "Magnetic field dependence of

- samples of nominal composition $\text{Bi}_{1.6}\text{Pb}_{0.4}\text{Sr}_2\text{Ca}_3\text{Cu}_4\text{O}_y(2234)$ prepared by various techniques,” *Journal of Alloys and Compounds*, vol. 239, no. 2, pp. 142–146, 1996.
- [16] H. B. Huang, G. F. de la Fuente, A. Sotelo, M. T. Ruiz, A. Larrea, L. A. Angurel and R. Navarro, “Ag/(Bi, Pb)-Sr-Ca-Cu-O superconducting tape processing-solid-state chemistry aspects,” *Solid State Ionics*, vol. 63–65, pp. 889–896, 1993.
- [17] N. Ghanzanfari, A. Kılıç, A. Gencer and H. Ozkan, “Effects of Nb_2O_5 addition on superconducting properties of BSCCO,” *Solid State Communications*, vol. 144, no. 5–6, pp. 210–214, 2007.
- [18] W. Zhu and P.S. Nicholson, “Atmosphere-temperature-time relationships for the formation of 110 K phase in the Bi-Pb-Sr-Ca-Cu-O superconductor system,” *Applied Physics Letters*, vol. 61, no. 6, pp. 717–719, 1992.
- [19] M. Borik, M. Chernikov, I. Dubov, V. Osiko, V. Veselago, Y. Yakowets and V. Stepankin, “Synthesis conditions superconduction properties of ceramic in the (Bi,Pb)-Sr-Ca-Cu-O system,” *Superconductor Science & Technology*, vol. 5, no. 3, pp. 151–155, 1992.
- [20] R. Mawassi, S. Marhaba, M. Roumié, R. Awad, M. Korek and I. Hassan, “Improvement of Superconducting Parameters of $\text{Bi}_{1.8}\text{Pb}_{0.4}\text{Sr}_2\text{Ca}_2\text{Cu}_3\text{O}_{10+\delta}$ Added with Nano-Ag,” *Journal of Superconductivity and Novel Magnetism*, vol. 27, no. 5, 1131–1142, 2014.
- [21] M. Roumié, S. Marhaba, R. Awad, M. Kork, I. Hassan and R. Mawassi, “Effect of Fe_2O_3 Nano-Oxide Addition on the Superconducting Properties of the (Bi, Pb)-2223 Phase,” *Journal of Superconductivity and Novel Magnetism*, vol. 27, no. 1, pp. 143–153, 2014.
- [22] F. Saad Oboudi, “Synthesis and magnetic properties of $\text{Bi}_{1.7}\text{Pb}_{0.3}\text{Sr}_2\text{Ca}_2\text{Cu}_3\text{O}_{10+\delta}$ added with nano Y,” *Journal of Superconductivity and Novel Magnetism*, vol. 30, no. 6, pp. 1473–1482, 2017.
- [23] N. A. A. Yahya, A. Al-Sharabi, N. Raihan Mohd Suib, W. S. Chiu and R. Abd-Shukor, “Enhanced transport critical current density of (Bi,Pb)-2223/Ag superconductor tapes added with nano-sized Bi_2O_3 ,” *Ceramics International*, vol. 42, no. 16, pp. 18347–18351, 2016.
- [24] S. Yavuz, O. Bilgili and K. Kocabas, “Effects of superconducting parameters of SnO_2 nanoparticles addition on (Bi, Pb)-2223 phase,” *Journal of Materials Science-Materials In Electronics*, vol. 27, no. 5, pp. 4526–4533, 2016.
- [25] H. Bagiah, S. A. Halim, S. K. Chen, K. P. Lim, and M. M. Awang Kechik, “Effects of rare earth nanoparticles ($\text{M}=\text{Sm}_2\text{O}_3, \text{Ho}_2\text{O}_3, \text{Nd}_2\text{O}_3$) addition on the microstructure and superconducting transition of $\text{Bi}_{1.6}\text{Pb}_{0.4}\text{Sr}_2\text{Ca}_2\text{Cu}_3\text{O}_{10+\delta}$ ceramics,” *Sains Malaysiana*, vol. 45, no. 4, pp. 643–651, 2016.
- [26] E. Akdemir, M. Pakdil, H. Bilge, M. F. Kahraman, E. Bekiroglu, G. Yildirim, Y. Zalaoglu, E. Doruk and M. Oz, “Degeneration of mechanical characteristics and performances with Zr nanoparticles inserted in Bi-2223 superconducting matrix and increment in dislocation movement and cracks propagation,” *Journal of Materials Science-Materials In Electronics*, vol. 27, no. 3, pp. 2276–2287, 2016.
- [27] S. E. Mousavi Ghahfarokhi, N. Manhoush and I. Kazeminezhad, “The role of PbO nanoparticles doping on the stability of Bi-2223 phase in $\text{Bi}_{2-x}\text{Pb}_x\text{Sr}_2\text{Ca}_2\text{Cu}_4\text{O}_y$ compounds,” *Journal of Superconductivity and Novel Magnetism*, vol. 29, no. 1, pp. 33–39, 2016.
- [28] U. Oztornaci and B. Ozkurt, “The effect of nano-sized metallic Au addition on structural and magnetic properties of $\text{Bi}_{1.8}\text{Sr}_2\text{Au}_x\text{Ca}_{1.1}\text{Cu}_{2.1}\text{O}_y$ (Bi-2212) ceramics,” *Ceramics International*, vol. 43, no. 5, pp. 4545–4550, 2017.
- [29] B. Akkurt and G. Yildirim, “Change of mechanical performance and characterization with replacement of Ca by Gd nanoparticles in Bi-2212 system and suppression of durable tetragonal phase by Gd,” *Journal of Materials Science: Materials in Electronics*, vol. 27, no. 12, pp. 13034–13043, 2016.

- [30] N. K. Saritekin, M. Pakdil, G. Yildirim, M. Oz and T. Turgay, "Decrement in metastability with Zr nanoparticles inserted in Bi-2223 superconducting system and working principle of hybridization mechanism," *Journal of Materials Science: Materials in Electronics*, vol. 27, no. 1, pp. 956–965, 2016.
- [31] A. Zelati, A. Amirabadizadeh, A. Kompany, H. Salamati and J. Sonier, "Critical current density and intergranular coupling study of the dysprosium oxide nanoparticle added $\text{Bi}_{1.6}\text{Pb}_{0.4}\text{Sr}_2\text{Ca}_2\text{Cu}_3\text{O}_y$ superconductor," *Journal of Superconductivity and Novel Magnetism*, vol. 27, no. 10, pp. 2185–2193, 2014.
- [32] N. A. A. Yahya and R. Abd-Shukor, "Effect of different nanosized MgO on the transport critical current density of $\text{Bi}_{1.6}\text{Pb}_{0.4}\text{Sr}_2\text{Ca}_2\text{Cu}_3\text{O}_{10}$ superconductor," *Journal of Superconductivity and Novel Magnetism*, vol. 27, no. 2, pp. 329–335, 2014.
- [33] A. Agail and R. Abd-Shukor, "Transport current density of $(\text{Bi}_{1.6}\text{Pb}_{0.4})\text{Sr}_2\text{Ca}_2\text{Cu}_3\text{O}_{10}$ superconductor added with different nanosized ZnO," *Applied Physics A-Materials Science & Processing*, vol. 112, no. 2, pp. 501–506, 2013.
- [34] W. Kong and R. Abd-Shukor, "Enhanced electrical transport properties of nano NiFe_2O_4 -added $(\text{Bi}_{1.6}\text{Pb}_{0.4})\text{Sr}_2\text{Ca}_2\text{Cu}_3\text{O}_{10}$ superconductor," *Journal of Superconductivity and Novel Magnetism*, vol. 23, no. 2, pp. 257–263, 2010.
- [35] H. Aydin, O. Cakiroglu, M. Nursoy and C. Terzioglu, "Mechanical and Superconducting Properties of the $\text{Bi}_{1.8}\text{Pb}_{0.35}\text{Sr}_{1.9}\text{Ca}_{2.1}\text{Cu}_3\text{Gd}_x\text{O}_y$ System," *Chinese Journal of Physics*, vol. 47, no. 2, pp. 192–206, 2009.
- [36] L. Bonoldi, G. L. Calestani, M. G. Francesconi, G. Salsi, M. Sparpaglione and L. Zini, "Structural stability of bismuth-based superconductors under heterovalent substitution," *Physica C*, vol. 241, no. 1–2, pp. 37–44, 1995.
- [37] C. Terzioglu, H. Aydin, O. Ozturk, E. Bekiroglu and I. Belenli, "The influence of Gd addition on microstructure and transport properties of Bi-2223," *Physica B*, vol. 403, no. 19–20, pp. 3354–3359, 2008.
- [38] M. Erdem, O. Ozturk, E. Yucel, S. P. Altintas, A. Varilci, C. Terzioglu and I. Belenli, "Effect of Gd addition on the activation energies of Bi-2223 superconductor," *Physica B*, vol. 406, no. 3, pp. 705–709, 2011.
- [39] K. Yoshida, H. Sasakura, S. Tsukui, T. Tabata, M. Adachi, R. Oshima and Y. Mizokawa, "Preparation of metastable Bi-2223 phase of $\text{Bi}_2(\text{Ln}_x\text{Ca}_{2-x})\text{Ca}_2\text{Cu}_3\text{O}_z$ thin films ($0.3 \leq x \leq 0.7$, Ln=Pr, Nd, Sm, Eu and Gd)," *Physica C*, vol. 377, no. 1–2, pp. 101–106, 2002.
- [40] C. Terzioglu, "Investigation of some physical properties of Gd added Bi-2223 superconductors," *Journal of Alloys and Compounds*, vol. 509, no. 1, pp. 87–93, 2011.
- [41] H. Aydin, A. Babanli, S. P. Altintas, E. Asikuzun, N. Soylu, O. Ozturk, M. Dogruer, C. Terzioglu and G. Yildirim, "Breaking point of the harmony between Gd diffused Bi-2223 slabs with diffusion annealing temperature," *Journal of Materials Science: Materials in Electronics*, vol. 24, no. 11, pp. 4566–4573, 2013.
- [42] O. Bilgili and K. Kocabas, "Effects of Gd substitution on magnetic, structural and superconducting properties of $\text{Bi}_{1.7-x}\text{Pb}_{0.3}\text{Gd}_x\text{Sr}_2\text{Ca}_2\text{Cu}_3\text{O}_y$," *Journal of Materials Science: Materials in Electronics*, vol. 26, no. 3, pp. 1700–1708, 2015.
- [43] G. Yildirim, Y. Zalaoglu, M. Akdogan, S. P. Altintas, A. Varilci and C. Terzioglu, "Investigation of Gd Addition Added on Magnetic and Structural Properties of $\text{Bi}_{1.8}\text{Pb}_{0.35}\text{Sr}_{1.9}\text{Ca}_{2.1}\text{Cu}_3\text{Gd}_x\text{O}_y$ Superconductors by ac Susceptibility," *Journal of Superconductivity and Novel Magnetism*, vol. 24, no. 7, pp. 2153–2159, 2011.
- [44] D. R. Mishra, "Gd-substituted Bi-2223 superconductor," *Pramana Journal of Physics*, vol. 70, no. 3, pp. 535–541, 2008.
- [45] R. Kalyanaraman, S. Oktyabrsky and J. Narayan, "The role of Ag in the pulsed laser growth of YBCO thin films," *Journal of*

- Applied Physics*, vol. 85, no. 9, pp. 6636–6641, 1999.
- [46] F. Rullier-Albenque, P. A. Vieillefond, H. Alloul, A. W. Tyler, P. Lejay and J. F. Marucco, “Universal T_c depression by irradiation defects in underdoped and overdoped cuprates,” *Europhysics Letters*, vol. 50, no. 1, pp. 81–87, 2000.
- [47] X. Xu, J. H. Kim, S. X. Dou, S. Choi, J. H. Lee, H. W. Park, M. Rindfleish and M. Tomsic, “A correlation between transport current density and grain connectivity in MgB_2/Fe wire made from ball-milled boron,” *Journal of Applied Physics*, vol. 105, no. 10, pp. 103913, 2009.
- [48] C. Autret-Lambert, B. Pignon, M. Gervais, I. Monot-Laffez, A. Ruyter, L. Ammor, F. Gervais, J. M. Bassat and R. Decourt, “Microstructural and transport properties in substituted $Bi_2Sr_2CaCu_2O_{8+\delta}$ modulated compounds,” *Journal of Solid State Chemistry*, vol. 179, no. 6, pp. 1698–1706, 2006.
- [49] S. B. Guner, O. Gorur, S. Celik, M. Dogruer, G. Yildirim, A. Varilci and C. Terzioglu, “Effect of zirconium diffusion on the microstructural and superconducting properties of $YBa_2Cu_3O_{7-\delta}$ superconductors,” *Journal of Alloys And Compounds*, vol. 540, pp. 260–266, 2012.
- [50] K. Kocabas, O. Ozkan, O. Bilgili, Y. Kadioglu and H. Yilmaz, “The Effects of Mg Substitution in Bi-2223 Superconductors,” *Journal of Superconductivity and Novel Magnetism*, vol. 23, no. 8, pp. 1485–1492, 2010.
- [51] D. M. Rao, T. Somaiah, V. Haribabu and Y. C. Venudhar, “Growth-kinetics of high- T_c and low- T_c phases in $Bi_{2-x}Pb_xCa_2Sr_2Cu_3O_y$ superconducting compounds,” *Crystal Research and Technology*, vol. 28, no. 3, pp. 285–298, 1993.
- [52] A. Ianculescu, M. Gartner, B. Despax, V. Bley, R. Th Lebey and M. Modreanu Gavrilă, “Optical characterization and microstructure of $BaTiO_3$ thin films obtained by RF-magnetron sputtering,” *Applied Surface Science*, vol. 253, no. 1, pp. 344–348, 2006.
- [53] A. I. Abou-Aly, S. A. Mahmoud, R. Awad and M. M. E. Barakat, “Electrical Resistivity and Magnetoresistance Studies of (Bi, Pb)-2223 Phase Substituted by Ru,” *Journal of Superconductivity and Novel Magnetism*, vol. 23, no. 8, pp. 1575–1588, 2010.
- [54] R. Shabna, P. M. Sarun, S. Vinu, A. Biju and U. Syamaprasad, “Doping controlled metal to insulator transition in the (Bi, Pb)-2212 system,” *Superconductor Science & Technology*, vol. 22, no. 4, pp. 045016, 2009.
- [55] S. Vinu, P. M. Sarun, R. Shabna, A. Biju and U. Syamaprasad, “Improved microstructure and flux pinning properties of Gd-substituted (Bi, Pb)-2212 superconductor sintered between 846 and 860 °C,” *Materials Letters*, vol. 62, no. 29, pp. 4421–4424, 2008.
- [56] P. M. Sarun, S. Vinu, R. Shabna, A. Biju, U. Syamaprasad, “Highly enhanced superconducting properties of Eu-doped (Bi, Pb)-2212,” *Materials Letters*, vol. 62, no. 17–18, pp. 2725–2728, 2008.
- [57] C. NguyenVanHuong, C. Hinnen and J. M. Siffre, “Superconductivity and X-ray photoelectron spectroscopy studies of $Bi_2Sr_{2-x}La_xCaCu_2O_{8+\delta}$,” *Journal of Materials Science*, vol. 32, no. 7, pp. 1725–1731, 1997.
- [58] P. M. Sarun, S. Vinu, R. Shabna, A. Biju and U. Syamaprasad, “Microstructural and superconducting properties of Yb-substituted (Bi, Pb)-2212 superconductor sintered at different temperatures,” *Journal of Alloys and Compounds*, vol. 472, no. 1–2, pp. 13–17, 2009.
- [59] A. Biju, P. M. Sarun, R. P. Aloysius and U. Syamaprasad, “Flux pinning properties of Yb substituted (Bi, Pb)-2212 superconductor,” *Journal of Alloys and Compounds*, vol. 454, no. 1–2, pp. 46–51, 2008.
- [60] S. Vinu, P. M. Sarun, A. Biju, R. Shabna, P. Guruswamy and U. Syamaprasad, “The effect of substitution of Eu on the critical current density and flux pinning properties of (Bi, Pb)-2212 superconductor,” *Superconductor Science & Technology*, vol. 21, no. 4, pp. 045001, 2008.
- [61] H. Wang, A. Serquis, B. Maiorov, L. Civale, Q. X. Jia, P. N. Arendt, S. R.

- Foltyn, J.L. Macmanus-driscoll and X. Zhang, "Microstructure and transport properties of Y-rich $\text{YBa}_2\text{Cu}_3\text{O}_{7-\delta}$ thin films," *Journal of Applied Physics*, vol. **100**, no. **5**, pp. 053904, 2006.
- [62] R. Shabna, P. M. Sarun, S. Vinu, A. Biju and U. Syamaprasad, "Charge carrier localization and metal to insulator transition in cerium substituted (Bi, Pb)-2212 superconductor," *Journal of Alloys and Compounds*, vol. 493, no. 1–2, pp. 11–16, 2010.
- [63] A. Yildiz, K. Kocabas and G. B. Akyuz, "Dependence of the Structural, Electrical and Magnetic Properties of $\text{YBa}_2\text{Cu}_3\text{O}_{7-\delta}$ Bulk Superconductor on the Ag Doping," *Journal of Superconductivity and Novel Magnetism*, vol. 25, no. 5, pp. 1459–1467, 2012.
- [64] B. F. Azzouz, A. Mchirgui, B. Yangui, C. Boulesteix and B. M. Salem, "Synthesis, microstructural evolution and the role of substantial addition of PbO during the final processing of (Bi, Pb)-2223 superconductors," *Physica C*, vol. 356, no. 1–2, pp. 83–96, 2001.
- [65] M. R. Persland, J. L. Tallon, R. G. Buckley, R. S. Liu and N. E. Floer, "General trends in oxygen stoichiometry effects on T_c in Bi and Tl superconductors," *Physica C*, vol. 176, no. 1–3, pp. 95–105, 1991.